# Supplementary Information for "Individual Closed-Loop Control of Micromotors by Selective Light Actuation"

David P. Rivas,[1] Max Sokolich,[1] and Sambeeta Das[1]
[1] *Department of Mechanical Engineering, Newark, DE, USA, 19716*

## I. LIST OF SUPPLEMENTARY VIDEOS

**Video S1:** Video showing the activation of a micromotor within a light "highway" in the shape of an "L". The micromotor was magnetically steered using an x-box joystick to remain inside the region. When the light was turned off, the micromotor halted its self-propulsion, as can be seen in the video. The smaller sized micromotors were used in this demonstration.
**Video S2:** Video showing the creation of a pattern of groups of micromotors using a localized "spotlight" which selectively activates individual micromotors independently. The micromotors were magnetically steered to the desired location.
**Video S3:** An example of closed-loop control of micromotors to create patterns of various shapes. A micromotor is selected and its desired final location is specified. The automated code then keeps the spotlight of light on the micromotor while also automatically magnetically steering it so that it reaches the intended final location. This is repeated with multiple micromotors to create the final pattern. The tracking algorithm displays a red circle around the selected micromotor while other objects it identifies in proximity are circled in blue. A yellow arrow points from the micromotor to the target location. Note that reflections of the light can sometimes be seen in the video but do not correspond to the actual location of the spotlight. The larger micromotors were used in this demonstration.

## II. METHODS

### A. Fabrication of micromotors

Micromotors of two different sizes were created. A solvent extraction/evaporation method was used to create the smaller light-actuated $TiO_2$ micromotors at an average diameter of 1.3 $\mu$m, following a previously stated procedure [1]. A mixture of tetrabutyl titanate (Sigma #244122) and ethanol was created at a 1 to 40 ratio. The mixture was stirred well and allowed to sit for one day before centrifuging at 7000 rpm (Eppendorf 5415) for 1 minute. The supernantant was discarded and the micromotors were rinsed two more times in DI water.

To create larger particles, a solvothermal method was used following the procedure in Ref. 2. A mixture of 1.3 mL titanium isopropoxide was mixed with 30 mL ethanol and 0.35 mL formic acid and placed in a Teflon-lined autoclave for approximately 12 hours at 150°C. The average diameter of these particles was measured to be 4.4 with a standard deviation of 1.4 $\mu$m.

Both the larger and smaller particles were washed and a glass vial containing the particles was placed on a hotplate at approximately 90°C to evaporate the liquid. Then, the dried particles were annealed in a furnace at 400°C for two hours to create the anatase phase. The particles were then suspended in ethanol and spread onto a glass slide. After the ethanol evaporated, the slides of the smaller particles were coated with 20 nm each of Ni/Fe alloy, Pt, and Ag by electron-beam evaporation, as described previously [3]. The larger particles were coated with a 20 nm layer of Ni.

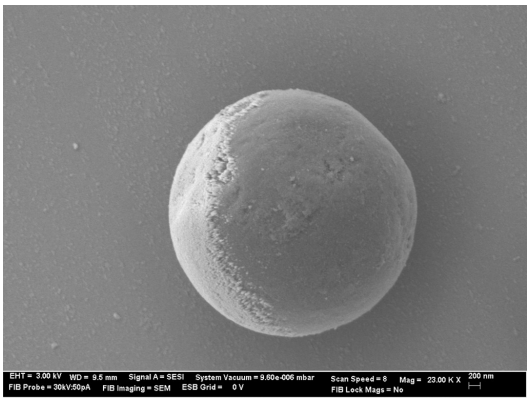


**Fig. S1.** SEM image of a $TiO_2$ micromotor half-coated with Ni.

### B. DMD system

UV light at 365 nm was produced by a digital micromirror device (DMD) (Mightex Polygon Pattern Illuminator) which illuminates the sample from below. The device provides precise spatial and temporal control of light with micron scale resolution. Mightex Polyscan software allows for any 2D binary image to be converted into a light pattern within a rectangular region within the field of view.

### C. Light Intensity

We measured the light intensity using a UV meter that was placed on the end of the objective lens. Because the DMD produces a small area of illumination, the entire

sensor was not illuminated, so we corrected the intensity reading by multiplying by ratio of the area of the sensor to the actual area of the illuminated region. We calculated the intensity at a range of light strengths at a full area of illumination and also for partial areas of illumination at max light strength. We found that the intensity was not noticeably changed when applying different areas of illumination. For example, applying a light region that was 1/4 the area of the full rectangle would produce nearly exactly 1/4 of the power, and hence equal intensity (power per unit area). It was possible to make this measurement down to areas a few times larger than the small disk of light that was used in the experiments. Using areas smaller than this resulted in a sensor reading that was too low to accurately compare to the readings at larger areas. Although we could not directly accurately measure the intensity of the small disk of light, the fact that the intensity was approximately constant as a function of area indicates that the small disk of light likely produces the same intensity as the larger rectangular area of illumination.

There was a decrease in the reading for small rectangles that were applied at the edges of the full rectangular region compared to the center (by about 30-35%), showing that the light intensity falls off somewhat from the center to the edges. If a similar effect is occurring in the case of a disk of light, this could explain why the micromotors move somewhat more slowly when illuminated by a disk compared to the full rectangular region, since they are not always in the center of the disk. It is also possible that the intensity of a small disk is in fact less than a larger area since we were unable to measure this directly. If neither of these is the reason for the lower speed, then perhaps there is some change in the self-electrophoretic propulsion that is responsible for the difference, although the exact mechanism for this is unclear.

Most of the experiments shown in this manuscript were performed with a 20x objective. The light intensity with a 50x objective increases by about 25/4 due to the decrease in area of the illuminated region while maintaining approximately the same power.

### D. Electromagnetic System

Magnetic fields were supplied with a three-axis electromagnetic system [4], which produces uniform magnetic fields in any direction. The amount of current passing through the coils, which sets the magnetic field strength, is controlled via a custom python program. Manual control of the magnetic fields is accomplished using an X-box controller joystick that interfaces with the software to produce the desired magnetic fields. The field strength at the center of the sample is approximately 5 mT.

### E. Experimental Setup and Procedures

To remove the micromotors from the glass slide, a small piece of lens tissue was wetted with water and wiped over the slide to pick up the $TiO_2$ micromotors. The lens tissue was placed in a 1.5 mL plastic tube with approximately 500 $\mu$L of DI water and shaken. The tissue was removed and the tube was sonicated for two minutes. Then 100 $\mu$L of the micromotor solution was added to a separate tube and hydrogen peroxide was added to the desired concentration. The solution was mixed and then a drop was placed on a coverslip on the microscope. Samples were observed using a Zeiss Axiovert 200 microscope with a 50x objective (Zeiss epiplan-neofluar 50x/0.8) and videos were recorded with an Amscope MU903-GS microscope digital camera.

### F. Closed-Loop Control Algorithm

A custom closed-loop algorithm written in Python was used in this work. The automated magnetic steering of the micromotors is described elsewhere in Sokolich *et al.*. Briefly, the code evaluates the average direction of motion of the micromotor over a short time period and determines the angular offset between this and the applied field. It then updates the orientation of the field to compensate for this offset, while also re-orientating the field in order to direct the micromotor toward the target location.

For automated light following of the UV spotlight, the light disk is first positioned in the DMD software such that the micromotor is illuminated, then a keystroke is used to signal the python code to drag the disk using the cursor in such a way as to compensate for the movement of the micromotor. The micromotor then moves by light actuation while being magnetically steered towards the final target location. To move a subsequent micromotor, a keystroke halts the light tracking of the previous micromotor and a different micromotor is selected as well as a new target location, repeating the process.

### G. Speed of Micromotors

The speed of the larger micromotors vs light intensity is shown in Fig. 2 of the main text. We also measured the speed of the smaller micromotors as a function of light intensity and the results are shown in Fig. S2.

Our measured average speeds of the smaller and larger micromotors are comparable to a previous report that used a very similarly designed $TiO_2$ micromotor with Pt and Ag coatings at 5% $H_2O_2$ and 600 $mW/cm^2$ light intensity [6]. Other reports have found higher or lower speeds with different designs and in different conditions [1, 7, 8]. We attribute these differences to surface roughness of the coatings which can effect the efficiency of

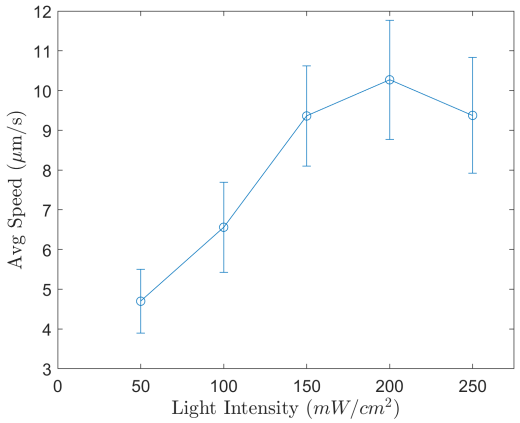


**Fig. S2.** The average speed of the smaller micromotors as a function of light intensity. The hydrogen peroxide concentration was 15%.

the catalytic reaction[6, 9, 10], the type of metal coating [7], the purity of the DI water used, the size of the particles[11, 12], and even the tilt angle of the micromotors [13].

### H. Particle Motion Without Light

When non-illuminated, the smaller particles undergo Brownian motion while the larger particles show some small Brownian motion but are mostly stationary. To quantify this, we measured their mean-squared-displacement (MSD) which we show in Fig. S3 along with linear fits to the data. As one can see from the plots, the larger particles move considerably less than the smaller particles when the light is off. The measured slope of the lines were $1.57 \pm 0.03$ $\mu m^2$/s for the smaller particles and $0.0306 \pm 0.0002$ $\mu m^2$/s for the larger particles.


[1] R. Dong, Q. Zhang, W. Gao, A. Pei, and B. Ren, Highly efficient light-driven tio2–au janus micromotors, ACS nano **10**, 839 (2016).

[2] C. Chen, F. Mou, L. Xu, S. Wang, J. Guan, Z. Feng, Q. Wang, L. Kong, W. Li, J. Wang, and Q. Zhang, Light-steered isotropic semiconductor micromotors, Advanced Materials **29**, 1603374 (2017).

[3] B. Wu, D. P. Rivas, and S. Das, Upstream mobility and swarming of light activated micromotors, Materials Advances (2024).

[4] M. Sokolich, D. Rivas, Y. Yang, M. Duey, and S. Das, Modmag: A modular magnetic micro-robotic manipulation device, MethodsX **10**, 102171 (2023).

[5] M. Sokolich, D. Rivas, Z. H. Shah, and S. Das, Automated control of catalytic janus micromotors, MRS Advances **8**, 1005 (2023).

[6] Z. Xiao, J. Chen, S. Duan, X. Lv, J. Wang, X. Ma, J. Tang, and W. Wang, Bimetallic coatings synergistically enhance the speeds of photocatalytic tio 2 micromotors, Chemical communications **56**, 4728 (2020).

[7] T. Maric, M. Z. M. Nasir, R. D. Webster, and M. Pumera, Tailoring metal/tio2 interface to influence motion of light-activated janus micromotors, Advanced Functional Materials **30**, 1908614 (2020).

[8] Q.-l. Wang, C. Wang, R.-f. Dong, Q.-q. Pang, and Y.-p. Cai, Steerable light-driven tio2-fe janus micromotor, Inorganic Chemistry Communications **91**, 1 (2018).

[9] U. Choudhury, L. Soler, J. G. Gibbs, S. Sanchez, and P. Fischer, Surface roughness-induced speed increase for active janus micromotors, Chemical communications **51**, 8660 (2015).

[10] A. M. Pourrahimi, K. Villa, C. L. Manzanares Palenzuela, Y. Ying, Z. Sofer, and M. Pumera, Catalytic and light-driven zno/pt janus nano/micromotors: switching of motion mechanism via interface roughness and defect tailoring at the nanoscale, Advanced Functional Materials **29**, 1808678 (2019).

[11] S. Ebbens, M.-H. Tu, J. R. Howse, and R. Golestanian, Size dependence of the propulsion velocity for catalytic janus-sphere swimmers, Physical Review E—Statistical, Nonlinear, and Soft Matter Physics **85**, 020401 (2012).

[12] P. M. Wheat, N. A. Marine, J. L. Moran, and J. D. Posner, Rapid fabrication of bimetallic spherical motors, Langmuir **26**, 13052 (2010).

[13] Z. Xiao, S. Duan, P. Xu, J. Cui, H. Zhang, and W. Wang, Synergistic speed enhancement of an electric-photochemical hybrid micromotor by tilt rectification, ACS nano **14**, 8658 (2020).

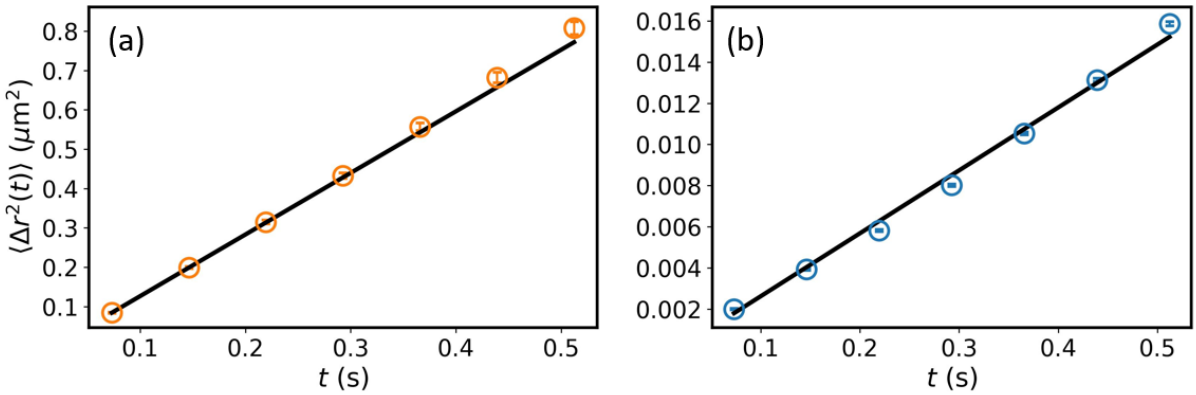


**Fig. S3.** MSDs of the small (a) and large (b) particles without light applied, along with fits to the data. The hydrogen peroxide concentration was 15%.